

Self-Sustained Collisional Drift-Wave Turbulence in a Sheared Magnetic Field

Bruce D. Scott

Max Planck Institut für Plasmaphysik, D8046 Garching bei München, Germany

(Received 6 July 1990)

Although collisional drift waves in a sheared slab configuration are linearly damped, it is found that the corresponding turbulence is self-sustaining if initialized at nonlinear amplitude. The influence of the free-energy source represented by the temperature and density gradients on the turbulent system involving bidirectional spectral energy transfer is responsible for this change of regime. Several important features of tokamak edge fluctuations are reproduced by these single-rational-surface nonlinear dynamics. As a result, drift-wave turbulence must still be considered as an underlying dynamic of anomalous transport in tokamak edges.

PACS numbers: 52.35.Kt, 52.35.Ra, 52.65.+z

It is a common perception in tokamak plasma physics that drift-wave turbulence cannot be the agent behind energy transport in tokamak edges.¹ That is, since the sheared slab modes are linearly stable² some interplay with toroidal effects is needed to provide a nonadiabatic electron response sufficient to drive them,^{3,4} and since the growth rates and/or mode widths of such linear waves fall rapidly with temperature, saturated fluctuation amplitudes would drop towards the edge regions in contrast to the observed rise.⁵ This thinking is based on linear mixing-length arguments⁶ or more sophisticated turbulent closure models⁷ which nevertheless require the presence of unstable modes. Further, conventional wisdom usually considers drift-wave electron dynamics as adiabatic, while the experimental evidence in tokamak edge regions indicates otherwise.^{1,5}

Before closing judgement on the viability of drift waves as an agent for transport, however, one should take into account the possibility of enhanced free-energy access by nonlinear processes, since the nonlinear mode structure of the turbulence is vastly different from that of linear drift waves. It was recently shown in the case of neglecting temperature fluctuations (referred to here as “pure ∇n ”) that the turbulence spontaneously self-organizes under the influence of both shear and density gradient to efficiently tap the free energy in the gradient.⁸ Nonlinear, nonadiabatic electron dynamics occurring near the mode resonant surface were responsible for this new regime. As a result, the external drive needed to support a turbulent state was much less than that needed to drive individual modes unstable, although a finite level was still needed in the pure- ∇n case.

Herein we consider the combined effects of the electron temperature and density dynamics, in closer correspondence to the realistic situation.⁹ The temperature is much freer than the density to have its relative phase with the potential set up by the turbulence independently of parallel dissipation, so its gradient is by far the stronger free-energy source. It is found that under its influence the turbulence needs no external drive at all to sustain itself at saturation, provided it is initialized at nonlinear amplitude. Further, with both gradients active as free-energy sources, the turbulence at saturation

reproduces many important features of observed tokamak edge fluctuations, most particularly the amplitude ordering, $e\tilde{\phi}/T > \tilde{n}/n > \tilde{T}/T$.

The fluidlike turbulence under study springs from the nonlinear collisional drift-wave system, whose linear aspects were studied previously.^{10,11} Collisional effects are important if the electron conduction channel width is as large as a typical gyroradius: $\Delta_D^2 > \rho_s^2$, where $\Delta_D = (\omega_*/k'_{\parallel} D_{\parallel})^{1/2}$ is the width of the region near the mode resonant surface within which the electron dynamics are nonadiabatic and thermal conduction does not effectively smooth out temperature variations. Here, $\omega_* = ck_0 T / eBL_T$ is the diamagnetic frequency, k_0 is the lowest wave number on a resonant surface, $D_{\parallel} = T/ne^2\eta_{\parallel}$, $\rho_s^2 = c^2 T \times M_i / e^2 B^2$, $k'_{\parallel} = k_0 / L_s$, and T is T_e . The dynamics in a 2D sheared slab are described by the electrostatic, cold-ion Braginskii equations,¹²

$$\eta_{\parallel} \tilde{J}_{\parallel} = (T/ne) \nabla_{\parallel} \tilde{n} + (\hat{a}/e) \nabla_{\parallel} \tilde{T} - \nabla_{\parallel} \tilde{\phi}, \quad (1)$$

$$d\tilde{\phi}/dt = 4\pi(v_A^2/c^2) \nabla_{\parallel} \tilde{J}_{\parallel}, \quad (2)$$

$$d\tilde{n}/dt = (cn'/B) \partial \tilde{\phi} / \partial y + (1/e) \nabla_{\parallel} \tilde{J}_{\parallel} - n \nabla_{\parallel} \tilde{u}_{\parallel}, \quad (3)$$

$$d\tilde{T}/dt = (cT'/B) \partial \tilde{\phi} / \partial y + \frac{2}{3} (\hat{a}T/ne) \nabla_{\parallel} \tilde{J}_{\parallel} - \frac{2}{3} T \nabla_{\parallel} \tilde{u}_{\parallel} + \kappa_{\parallel} \nabla_{\parallel}^2 \tilde{T}, \quad (4)$$

$$nM_i d\tilde{u}_{\parallel}/dt = -T \nabla_{\parallel} \tilde{n} - n \nabla_{\parallel} \tilde{T} + nM_i \mu_{\parallel} \nabla_{\parallel}^2 \tilde{u}_{\parallel}. \quad (5)$$

Standard notation is used here, with $d/dt = \partial/\partial t + (c/B) \nabla_z \times \nabla \tilde{\phi} \cdot \nabla$, $\nabla_{\parallel} = (x/L_s) \partial/\partial y$, $\kappa_{\parallel} = 1.07 D_{\parallel}$, and $\hat{a} = 1.71$. In rough correspondence to ion Landau damping, the parallel viscosity μ_{\parallel} is set to $T/M_i \omega_*$. The system is 2D (x and y), with $\mathbf{B} = B[\nabla_z + (x/L_s) \nabla_y]$ and the gradients, n' and T' , in the direction of $-\nabla x$. As is customary in treatments of electron drift-wave dynamics, no attempt is made to address ion-temperature effects. The time-dependent thermal force¹³ is also neglected.

Equations (1)–(5) are solved numerically—pseudospectral in y , finite differenced in x , implicit for ∇_{\parallel}^2 terms, predictor-corrector for advection, and with a small artificial damping in the form of a hyperviscosity, $-\mu_{\perp} \nabla_{\perp}^4$, added to each equation—by a method which passed linear as well as nonlinear tests.^{9,14} The grid in x runs from $-20\rho_s$ to $20\rho_s$, and the 85 Fourier modes in y range from $k_y \rho_s = 0.07$ to 5.95. The parameter control-

ling collisionality is

$$C = \Delta_D^2 / \rho_s^2 = 0.51 (v_e / \omega_*) (m_e / M_i) (L_s^2 / L_T^2),$$

which is set to 10 (see ASDEX parameters below). Specification is completed with $L_s / L_T = 10$ and $Tn' / nT' = 1$. A run is initialized with a broadband, random phase⁸ $\tilde{n}/n = e\tilde{\phi}/T$ at an rms amplitude of $1.5\rho_s/L_T$, with $\tilde{T} = \tilde{u}_{\parallel} = 0$, and allowed to evolve self-consistently.

The system is diagnosed with the fluctuation energy:

$$E = \frac{1}{2} \langle |\rho_s \nabla_{\perp} e\tilde{\phi}/T|^2 + |\tilde{n}/n|^2 + \frac{3}{2} |\tilde{T}/T|^2 + |\tilde{u}_{\parallel}/c_s|^2 \rangle,$$

where $c_s = (T/M_i)^{1/2}$ and the angular brackets indicate integrations over all space. The energy evolves as

$$(2E)^{-1} \partial E / \partial t = \Gamma_t + \Gamma_n - \Gamma_c - \Gamma_k - \Gamma_s, \quad (6a)$$

with sources and sinks given by

$$2E\Gamma_t \equiv \frac{3}{2} (1/TL_T) \langle \tilde{T} \tilde{v}_x \rangle, \quad 2E\Gamma_n \equiv (1/nL_n) \langle \tilde{n} \tilde{v}_x \rangle,$$

$$2E\Gamma_c \equiv D_{\parallel} \langle |\nabla_{\parallel} (\hat{a} \tilde{T}/T + \tilde{n}/n - e\tilde{\phi}/T)|^2 \rangle, \quad (6b)$$

$$2E\Gamma_k \equiv \frac{3}{2} \kappa_{\parallel} \langle |\nabla_{\parallel} \tilde{T}/T|^2 \rangle, \quad 2E\Gamma_s \equiv \mu_{\parallel} \langle |\nabla_{\parallel} \tilde{u}_{\parallel}/c_s|^2 \rangle,$$

where $\tilde{v}_x = -(c/B) \partial \tilde{\phi} / \partial y$. These are free-energy access from temperature (Γ_t) and density (Γ_n) gradients, and collisional (Γ_c and Γ_k) and sound-wave (Γ_s) dissipation. It is important to note that all of these Γ 's are zero in the initialization, allowing self-consistent evolution to determine their form and size in the saturated state. The mismatch in Eq. (6), most of which is due to the artificial damping, gives the error. This error was measured below $10^{-2} \omega_*$, i.e., lower than Γ_s and 2 orders down from Γ_t . From Fig. 1, we can see the turbulence in a very robust saturated state, with the rms amplitudes [1(a)] near Δ_D/L_T for $e\tilde{\phi}/T$, \tilde{n}/n , and \tilde{T}/T , in descending order, and higher than their initial levels. The energetics [1(b)] show that Δ_D -layer processes are dominant, with a balance between free-energy feed and collisional dissipation describing nearly all the source-sink flow: $\Gamma_t + \Gamma_n \approx \Gamma_c + \Gamma_k$. The sound-wave damping rate is smaller, since nonlinear mode coupling and not the parallel viscosity is responsible for mode localization.^{8,15}

The sheared-slab drift-wave system, Eqs. (1)-(5), admits no linear instabilities, the linear waves being damped by collisional dissipation ($\nabla_{\parallel} \tilde{J}_{\parallel}$ and κ_{\parallel} terms) and coupling to shear-damped parallel ion motion.^{10,11} Nevertheless, there remains the potent free-energy sources represented by the gradients in density and temperature. It is thereby clear that the access mechanism for self-sustained turbulence must be inherently nonlinear, and that spectral transfer dynamics must play a decisive role. On first sight, however, one might expect a randomly turbulent bath of fluctuations to tend towards a zero average correlation between any two independent fields, e.g., \tilde{T} and \tilde{v}_x , so that a positive one would depend on a linear instability. The reality, on the other hand, is that both the gradients and the shear conspire to keep Γ_n and Γ_t at the levels seen in Fig. 1.

The basis for the establishment of positive $\langle \tilde{T} \tilde{v}_x \rangle$ is a homogeneous process, which is able to act in and is

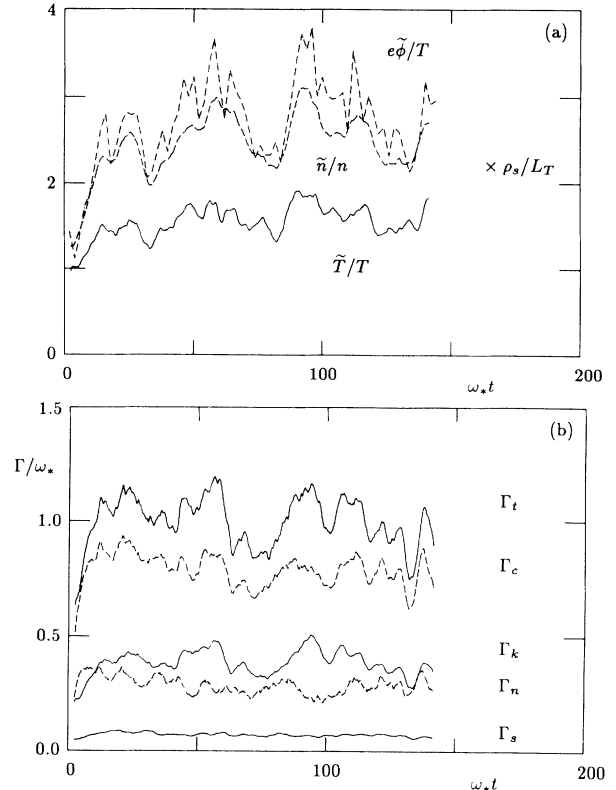


FIG. 1. (a) Evolution of the fluctuation amplitudes in units of ρ_s/L_T , showing growth from the initial level of 1.5 and saturation. (b) Evolution of the source and sink terms, defined in the text, showing vigorous transfer between free-energy feed (Γ_t and Γ_n) and collisional dissipation (Γ_c and Γ_k). Losses in parallel ion motion (Γ_s) are comparatively small. The curves have been smoothed within a window of $\omega_* \Delta t = 2$.

confined to the hydrodynamic layer, since there and only there are the parallel electron dynamics weak in comparison to turbulent advection. In a hydrodynamic context the dynamics of $\tilde{\phi}$ are those of a 2D fluid, while \tilde{n} and \tilde{T} are passively advected. Hence, the cascade tendencies are opposite—inverse for the former and direct (to small scales) for the latter.^{8,16} Considering the \tilde{n} or \tilde{T} separately, the energy balance for a batch of modes near inverse scale k is struck between input due to cascade from larger scales, output by cascade to smaller scales, and exchange with the gradient depending on the sign of the correlation with down-gradient flow (\tilde{v}_x). Clearly, a positive correlation in the ensemble average is favored since it is preferentially driven by the free-energy source. Evaluation of this energy balance for strong, homogeneous turbulence was carried out in Ref. 7, with the result that the free-energy feed-rate spectrum should be proportional to \tilde{v}_k/k , with \tilde{v}_k an rms amplitude. Simulation of the homogeneous model supported this physical picture by showing the feed-rate spectrum to take this form.

The second actor, the shear, confines such a homogeneous process to the hydrodynamic layer since beyond this the parallel dynamics destroy the necessary indepen-

dence of the fields ($\tilde{\phi}$ and either \tilde{n} or \tilde{T}). The layer thickness Δ_D thereby becomes the largest available scale for efficient free-energy feed. The shear also has the effect of channeling the Δ_D -size fluctuations, which cannot leave the layer. The inverse-cascade tendency of the $\tilde{\phi}$ puts much of its energy into low k , but these large-scale flows can only dig temperature and density fluctuations out of the gradients within the layer. The signature is a strong enhancement in the population of Δ_D -sized fluctuations. Since these must spend their lifetimes in the layer, they can only decorrelate in the y direction, an inefficient process, and linear coupling through the parallel dynamics puts some of their energy back into the $\tilde{\phi}$. The result is an overall structure, shown in Fig. 2, characterized by a predominance of Δ_D -sized fluctuations and flows whose phases are locked in by the large-scale flows which lead to their existence. Since so much of Γ_i comes from the two groups of fluctuations near $k_{0y} = \pi$ and 1.5π , it can be argued that this "self-organization"⁸ is the dominant process behind it.

Identification of this structure comes from the 2D power spectrum $S(k_y, \omega)$ for the \tilde{T} , shown in Fig. 3(b). It is immediately seen that all of the intermediate- to small-scale activity lies on the linear dispersion curve $[\omega_L$, found from linearizations of Eqs. (1)-(5)], indicating turbulence with no special phase behavior—the dispersion ($\omega/k_y \neq \text{const}$) shows that the Δ_D -sized fluctuations cannot be coherent structures. The longer wavelengths, however, are at least consistent with phase locking. Although in the present case the turbulent amplitude is high enough to mask out a clear identification, it has been made in the pure- ∇n case.⁸ As in that previous study, the time scale of the peak frequency for the

lowest k_y corresponds closely with the scale of temporal fluctuations in Γ_i and Γ_n in Fig. 1. Further reestablished is that the long-wavelength activity is entirely contained in this feature in $S(k_y, \omega)$ which lies wholly below the linear dispersion curve. This tells us the free-energy feed Γ_i is being mediated through long-lived, self-organized structure represented by the groups of Δ_D -sized fluctuations discussed above. Finally, we note that the total-input-rate spectrum [Fig. 3(a)], $\Gamma = \Gamma_i + \Gamma_n - \Gamma_c - \Gamma_k - \Gamma_s$, has the same form as that inferred from TEXT measurements: a peak at intermediate scale (here, Δ_D) with sinks to longer as well as shorter wavelengths.¹⁷

As for the relevance of collisional drift-wave turbulence to tokamaks, a good example is the edge region of Ohmically heated ASDEX plasmas,¹⁸ where the parameter C is given by

$$C = 5 \left(\frac{100 \text{ eV}}{T} \right)^{5/2} \left(\frac{L_s}{240 \text{ cm}} \right)^2 \left(\frac{10 \text{ cm}}{L_T} \right) \left(\frac{B}{20 \text{ kG}} \right) \times \left(\frac{n}{10^{13} \text{ cm}^{-3}} \right) \left(\frac{10}{m} \right) \left(\frac{r_0}{36 \text{ cm}} \right),$$

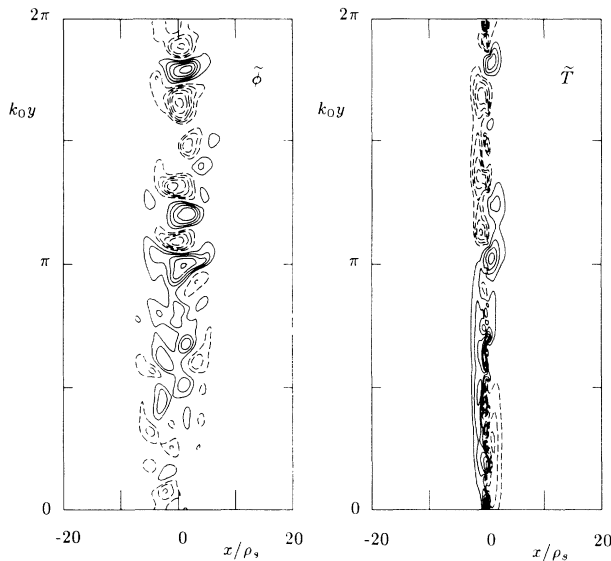


FIG. 2. Contours of $\tilde{\phi}$ and \tilde{T} at $\omega_* t = 100$, showing the phase-locked relation between flow vortices and Δ_D -sized temperature fluctuations. Solid lines are positive; dashed lines, negative. Sense of flow is clockwise around a $\tilde{\phi}$ maximum.

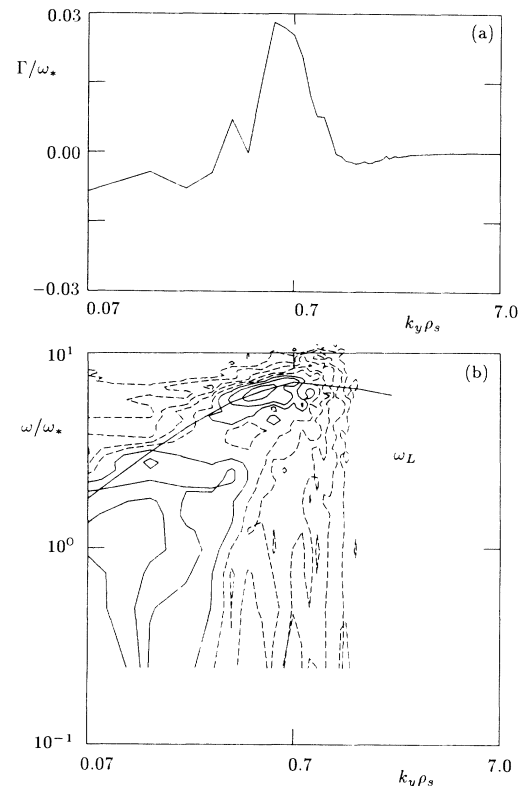


FIG. 3. (a) Net input (source-sink) rate. (b) Power spectrum $S(k_y, \omega)$ of the temperature fluctuations over the interval $60 < \omega_* t < 140$. The contour scale is logarithmic, with a factor of $10^{1/4}$ as the interval. Intermediate-scale activity is on the linear dispersion curve (ω_L), but long-wavelength activity lies entirely below it. Compare (b) with (a). Peaks in both these measurements are well to the left of $k_y/\rho_s = 1$, cementing Δ_D (here about $3\rho_s$) as the preferred scale.

with m the lowest poloidal mode number on the resonant surface located at minor radius r_0 . Study of the pure- ∇n case showed that the dynamics in the hydrodynamic layer play a dominant role in the system energetics even for the marginal case of $C=1$.⁸ The results given in this work are to be considered valid for strict comparison to observations if neighboring Δ_D 's (adjacent m numbers at same n) do not overlap. With the toroidal definition, $k_{\parallel}(m,n)=(nq-m)/qR$, the separation is $X=r_0/m\hat{s}$, with $\hat{s}=rq'/q$ the shear parameter. In the code, measured mode widths show the Δ_D -sized fluctuations—the random, isotropic component—in marginal overlap (mode width $\Delta k_y \approx 1/\hat{s}k_y$ for temperature and nonadiabatic density) but the long wavelengths—the coherent structures—are not, a situation entirely compatible with the 2D self-organization process (note that k_0 determines Δ_D). For $m=50$ modes on ASDEX (above parameters), X is about $10\rho_s$, so the Δ_D 's are well separated. On TEXT near the limiter, by contrast, $X \sim \Delta_D$, so the layers marginally overlap. In the 15-eV scrape-off layer for both machines, the entire region is hydrodynamic, which would explain the evidence from probes that particle-flux “convection” can account for the energy flux.¹⁹ Analysis of TEXT observations suggests that this ceases to be so inward of about 25 cm (Fig. 2 of Ref. 5), consistent with a supposed transition between overlap and nonoverlap of neighboring hydrodynamic layers. Indeed, the case of $\Gamma_t > \Gamma_n$ has been listed as an important observational constraint concerning “what theory must explain.”²⁰

These results show that strong turbulence near the mixing level is a natural result in a magnetically sheared plasma with a moderate temperature gradient, completely irrespective of linear stability since the mechanisms of free-energy access, source-sink transfer, and mode localization are all inherently nonlinear. The model given here reproduces several features of observed tokamak edge fluctuations:^{1,5,17,20} (a) $e\phi/T > \tilde{n}/n > \tilde{T}/T$; (b) $\Gamma_t > \Gamma_n$ where Δ_D overlap is not suspected; (c) bidirectional energy transfer out of a source range in k_y space; and, (d) fluctuation activity well to the long-wavelength side of $k_y\rho_s=1$. In the first, $e\tilde{\phi}/T$ is largest because although $\tilde{\phi}$ is not directly driven, it is coupled to both driven fields by the shear. In the pure- ∇n case, with only one driven field present, $e\phi/T$ was smaller than \tilde{n}/n .⁸ The next largest is \tilde{n}/n since being partially adiabatic its level is heavily influenced by that of $e\tilde{\phi}/T$. The second feature is due to the fact that \tilde{T} is forced merely to vanish at the edge of the hydrodynamic layer by thermal conduction (only \tilde{T} feels both Γ_k and Γ_c), while \tilde{n} is forced to track $\tilde{\phi}$ by resistive dissipation, i.e., merge into adiabaticity. The \tilde{T} are thereby left freer to directly correlate with \tilde{v}_x (i.e., poloidal electric field), as suggested by observations.¹⁷ The third feature is a result of both cascade tendencies being present—inverse for $\tilde{\phi}$ and direct for \tilde{n} and \tilde{T} —and of shear-induced coupling at all scales. The last feature results from $\Delta_D > \rho_s$, i.e., $C > 1$

in the edge regions of TEXT and ASDEX, from which the data come. Besides the fact of self-sustained turbulence (with a nonlinear start provided automatically by the turbulent buildup phase of the discharge), the first two of these, (a) and (b), could not have resulted from a pure- ∇n model. Moreover, if the fluctuation amplitude does turn out to scale with Δ_D/L_T , a rising edge-ward trend would result, since $\Delta_D \propto T^{-3/4}$. Further work is required to confirm this, but this work as well as Ref. 7 confirm Δ_D as the relevant cross-field scale, and a rising trend is at least to be expected. These results suggest persuasively that collisional drift-wave turbulence stands as a viable candidate for the underlying dynamic of edge turbulence in small- to medium-sized tokamaks.

I would like to thank D. Ross, E. Holzhauser, Ch. Ritz, R. Waltz, S. Cowley, J. Krommes, and M. Ottaviani for useful and stimulating discussions. This work was supported by the Max Planck Gesellschaft.

¹A. Wooton *et al.*, University of Texas, Austin, Fusion Research Center Report No. 340, 1989 (unpublished).

²D. W. Ross and S. M. Mahajan, *Phys. Rev. Lett.* **40**, 324 (1978); K. T. Tsang, P. J. Catto, J. C. Whitson, and J. Smith, *Phys. Rev. Lett.* **40**, 327 (1978).

³C. S. Liu, M. N. Rosenbluth, and W. M. Tang, *Phys. Fluids* **19**, 1040 (1976).

⁴L. Chen and C. Z. Cheng, *Phys. Fluids* **23**, 2242 (1980).

⁵Ch. Ritz *et al.*, *Phys. Rev. Lett.* **62**, 1844 (1989).

⁶W. M. Tang, *Nucl. Fusion* **26**, 1605 (1986).

⁷P. W. Terry and P. H. Diamond, *Phys. Fluids* **28**, 1419 (1985).

⁸Bruce D. Scott, H. Biglari, P. W. Terry, and P. H. Diamond, *Phys. Fluids B* (to be published).

⁹A completely detailed version of this work including the relationship to rippling modes is now under preparation.

¹⁰J. F. Drake and A. B. Hassam, *Phys. Fluids* **24**, 1262 (1981).

¹¹A. B. Hassam and J. F. Drake, *Phys. Fluids* **26**, 133 (1983).

¹²S. I. Braginskii, in *Reviews of Plasma Physics*, edited by M. A. Leontovich (Consultants Bureau, New York, 1965), Vol. 1, p. 205.

¹³A. B. Hassam, *Phys. Fluids* **23**, 2493 (1980).

¹⁴Bruce D. Scott, *J. Comput. Phys.* **78**, 114 (1988).

¹⁵D. Biskamp and M. Walter, *Phys. Lett. A* **109**, 34 (1985).

¹⁶F. Y. Gang, B. D. Scott, and P. H. Diamond, *Phys. Fluids B* **1**, 1331 (1989).

¹⁷Ch. P. Ritz, E. J. Powers, and R. D. Bengston, *Phys. Fluids B* **1**, 153 (1989).

¹⁸L. Gianonne, Max Planck Institut Plasmaphysik Report No. III/125 (unpublished). Parameters from Ohmically heated phase of shot No. 18041 at $r=36$ cm (separatrix at 40).

¹⁹R. D. Bengston *et al.*, in *Proceedings of the Seventeenth European Physical Society Conference on Controlled Fusion and Plasma Heating, Amsterdam, 1990* (European Physical Society, Petit-Lancy, 1990), p. 1460.

²⁰J. Hugill, in *Proceedings of the Joint Varenna-Lausanne International Workshop, August 1990*, edited by J. Vaclavik, F. Troyon, and E. Sindoni (Editrice Compostori, Bologna, to be published).